TU Delft

Delft University of Technology

Synthesis of Quasi-Modular Circularly Polarized 5G Base Station Antenna Arrays Based on Irregular Clustering and Sequential Rotation

Aslan, Y.; Puskely, J.; Roederer, A.G.; Yarovoy, Alexander

DOI
10.1002/mop.32735

Publication date
2020

Document Version
Final published version

Published in
Microwave & Optical Technology Letters

Citation (APA)
Aslan, Y., Puskely, J., Roederer, A. G., & Yarovoy, A. (2020). Synthesis of Quasi-Modular Circularly Polarized 5G Base Station Antenna Arrays Based on Irregular Clustering and Sequential Rotation. *Microwave & Optical Technology Letters*, *63*(4), 1278-1285. https://doi.org/10.1002/mop.32735

Important note
To cite this publication, please use the final published version (if applicable).
Please check the document version above.

Copyright
Other than for strictly personal use, it is not permitted to download, forward or distribute the text or part of it, without the consent of the author(s) and/or copyright holder(s), unless the work is under an open content license such as Creative Commons.

Takedown policy
Please contact us and provide details if you believe this document breaches copyrights.
We will remove access to the work immediately and investigate your claim.

This work is downloaded from Delft University of Technology.
For technical reasons the number of authors shown on this cover page is limited to a maximum of 10.

Received: 7 August 2020

DOI: 10.1002/mop.32735

WILEY

RESEARCH ARTICLE

Synthesis of quasi-modular circularly polarized 5G base station antenna arrays based on irregular clustering and sequential rotation

Yanki Aslan | **Jan Puskely** | **Antoine Roederer** | **Alexander Yarovoy**

Department of Microelectronics, Microwave Sensing, Signals and Systems Group, Delft University of Technology, Delft, The Netherlands

Correspondence
Yanki Aslan, TU Delft, Faculty of Electrical Engineering, Mathematics and Computer Science, HB 21, Mekelweg 4, 2628 CD Delft, The Netherlands.
Email: y.aslan@tudelft.nl

Funding information
Nederlandse Organisatie voor Wetenschappelijk Onderzoek, Grant/Award Number: 15590; NXP Semiconductors

Abstract

An unconventional, yet quasi-modular base station phased array architecture synthesis technique is proposed for multiuser fifth-generation applications. By keeping uniform amplitudes and linearly progressing phases at the elements of an optimal irregular array, power-efficient side lobe suppression is achieved for effective inter-user interference mitigation. The layout irregularity is achieved within a slice of an array, which is repeated rotationally. The sequential rotation technique is applied to obtain modularity and improve the circular polarization characteristics. A modified k-means clustering algorithm is used to form the optimal subarrays. The simulation results indicate that the proposed quasi-modular topologies provide a good compromise between the side lobe performance and integrated array design complexity.

KEYWORDS

antenna optimization, clustered arrays, fifth-generation, irregular architectures, sequential rotation

1 | INTRODUCTION

In space division multiplexing for fifth-generation (5G),[1] the inter-beam interference plays a crucial role in the performance of the communication network. Therefore, while serving a user, the undesired radiation toward the other simultaneous co-frequency users (i.e., side/grating lobes) must be sufficiently suppressed.

Element amplitude, phase, and position control/optimization are the commonly used array synthesis techniques to improve the radiation pattern characteristics and reduce the interference levels.[2-7] Among all techniques, the most power-efficient[1]way to decrease the side lobe levels (SLLs) is to keep uniform excitation amplitudes with linearly progressing phases, while optimizing the element positions.[8] If this is done on a fixed grid, the method is called array thinning.[9,10] The major disadvantage of a thinned array is that its SLL lowering capability is very limited, especially for wide-angle scanning, unless the array is made large enough.[11] A more flexible approach is to obtain space/density tapering by performing a gridless element position optimization.[12,13] A new gridless array layout optimization algorithm has recently been introduced by the authors[14,15] so as to synthesize the optimal multibeam irregular 5G base station arrays with the lowest SLLs. Complementary to this research, the system advantages (in terms of better quality-of-service, reduced processing burden and improved cooling capacity) of the proposed irregular arrays over the conventional regular counterparts have been stated in the recent literature.[16,17]

The major issue with the fully aperiodic integrated antennas is that they are hard to realize and use in practice, since the circuit routing and array calibration may become very complex. Therefore, to maintain the feasibility of array fabrication and reliability of operation, the industry prefers to have more modular layouts, which comes at the expense of increased SLLs.

One way to achieve modularity is to use irregular-shaped subarray partitioning and tiling. Many different subarray architectures and tiling strategies have been proposed in the literature.[18-23] Another, and a more straightforward, way to achieve modularity is to enforce a layout symmetry in the beginning of the element position optimization procedure, as proposed in the literature[24] for position-amplitude controlled arrays. A similar strategy is used in this article for position-only optimized arrays for power-efficient 5G antenna systems.

This is an open access article under the terms of the Creative Commons Attribution-NonCommercial License, which permits use, distribution and reproduction in any medium, provided the original work is properly cited and is not used for commercial purposes.
© 2020 The Authors. *Microwave and Optical Technology Letters* published by Wiley Periodicals LLC

In the aperiodic layouts with enforced symmetry, the modularity can be based on an N-th order rotational one for which only a slice (of $1/N$-th) of the total array is to be optimized. Besides the advantage regarding the reduced computational efforts, sequentially rotated arrays[25] allow us to synthesize circularly polarized (CP) arrays in an elegant way (using either CP or densely packed linearly polarized [LP] elements[26,27]) with low-cross-polarization in the main beam, reduced mutual coupling and wide axial ratio (AR) bandwidth.[28-31] Note that CP solutions may be preferable in mm-wave wireless communication systems since the single LP alternatives would need accurate polarization alignment between the base station and the users.[29]

In this article, we combine, for the first time, the irregular array layout design approach with the sequential rotation technique in order to synthesize novel quasi-modular integrated multibeam CP 5G base station antennas with the optimal power efficiencies and relatively low SLLs. Note that although demonstrated for CP arrays, the proposed method can also be straightforwardly applied to LP arrays with the proper element center adjustments.

The rest of the article is organized as follows. Section 2 formulates the optimization problem. Section 3 presents the simulation settings. The simulation results are given in Section 4. Finally, Section 5 presents the conclusions.

2 | PROBLEM FORMULATION

In this study, the element positions are optimized by applying the iterative convex position perturbation technique,[13,15] with an additional constraint on the layout symmetry. The optimization goal is to minimize the maximum SLL inside a predefined angular sector for a beam, which is freely scanned within that sector (i.e., multibeam optimization[24]). The proposed method is an extension of the aperiodic array synthesis technique,[15] with the novel introduction of the layout symmetry and sequential rotation. Therefore, as compared to the relevant array synthesis literature, it possesses all the advantages and assets of the convex optimization technique presented by the authors[15] (in terms of joint capabilities on uniform-amplitude excitation, element spacing control, multibeam optimization, powerful SLL suppression, and computational efficiency). Interested readers are referred to the comparative examples,[15] which clearly show the superior performance of the technique exploited in this article.

Let us consider a M-element uniformly excited planar array with a rotational symmetry of order N. Assume that there are P elements in the first slice[2] of the array (i.e., $M = NP$). At each iteration of the algorithm, the P elements are slightly moved along the $x-$ and $y-$directions by an amount given by the optimization parameters l and h, respectively.

The locations of the elements in the first slice at the i-th iteration of the algorithm and the corresponding position perturbations are defined as

$$\begin{aligned} \mathbf{x}^{1,i} &= \left[x_1^i\, x_2^i \ldots x_p^i\right]^T \\ \mathbf{y}^{1,i} &= \left[y_1^i\, y_2^i \ldots y_p^i\right]^T \\ \mathbf{l}^{1,i} &= \left[l_1^i\, l_2^i \ldots l_p^i\right]^T \\ \mathbf{h}^{1,i} &= \left[h_1^i\, h_2^i \ldots h_p^i\right]^T \end{aligned}, \tag{1}$$

where in $\{\mathbf{x}, \mathbf{y}, \mathbf{l}, \mathbf{h}\}^{a,b}$, a labels the slice and b shows the iteration number. T denotes the vector transpose operation. Let us form the complex vectors $\mathbf{z}^1$ and $\mathbf{q}^{1,i}$ as

$$\begin{aligned} \mathbf{z}^{1,i} &= \mathbf{x}^{1,i} + j\mathbf{y}^{1,i} \\ \mathbf{q}^{1,i} &= \mathbf{l}^{1,i} + j\mathbf{h}^{1,i} \end{aligned}. \tag{2}$$

In this case, the element locations and position perturbations at the slice $n = 2, \ldots$, are given by

$$\begin{aligned} \mathbf{x}^{n,i} &= \Re\left\{\mathbf{z}^{1,i}\exp\left(j\frac{2\pi}{N}(n-1)\right)\right\} \\ \mathbf{y}^{n,i} &= \left\{\mathbf{z}^{1,i}\exp\left(j\frac{2\pi}{N}(n-1)\right)\right\} \\ \mathbf{l}^{n,i} &= \Re\left\{\mathbf{z}^{1,i}\exp\left(j\frac{2\pi}{N}(n-1)\right)\right\} \\ \mathbf{h}^{n,i} &= \left\{\mathbf{q}^{1,i}\exp\left(j\frac{2\pi}{N}(n-1)\right)\right\} \end{aligned}, \tag{3}$$

where $\Re$ and $\Im$ gives the real and imaginary parts of the vectors. For the overall array, the element locations at the i-th iteration are given by

$$\begin{aligned} \mathbf{x}^i &= \left[\mathbf{x}^{1,i};\ \ldots;\ \mathbf{x}^{n,i};\ \ldots;\ \mathbf{x}^{N,i}\right] \\ \mathbf{y}^i &= \left[\mathbf{y}^{1,i};\ \ldots;\ \mathbf{y}^{n,i};\ \ldots;\ \mathbf{y}^{N,i}\right] \end{aligned}, \tag{4}$$

which can also be expressed as:

$$\begin{aligned} \mathbf{x}^i &= \left[\mathbf{x}^{1,i-1} + \mathbf{l}^{1,i};\ \ldots;\ \mathbf{x}^{n,i-1} + \mathbf{l}^{n,i};\ \ldots;\ \mathbf{x}^{N,i-1} + \mathbf{l}^{N,i}\right] \\ \mathbf{y}^i &= \left[\mathbf{y}^{1,i-1} + \mathbf{h}^{1,i};\ \ldots;\ \mathbf{y}^{n,i-1} + \mathbf{h}^{n,i};\ \ldots;\ \mathbf{y}^{N,i-1} + \mathbf{h}^{N,i}\right] \end{aligned}, \tag{5}$$

where $(i-1)$ denotes the previous iteration with known element locations.[3] The vectors $\mathbf{l}^{1,i}$ and $\mathbf{h}^{1,i}$ contain the $2p$ different parameters to be optimized at the iteration-i. Note that the resulting $(Mx1)$ vectors $\mathbf{x}^i$ and $\mathbf{y}^i$ contain all the element locations at the i-th iteration.

If the position perturbations are sufficiently small, that is, $|\mathbf{l}, \mathbf{h}^{1,i}| \ll \lambda/2\pi$, the far field expression can be linearized around the element locations.[13] Thus, the uv-plane far field expression at the i-th iteration for a scanned beam $s = 1, \ldots, S$ can be approximated as

$$f^{i,s}_{l_m,h_m}(u,v)\approx\frac{1}{M}\sum_{m=1}^{M}E^i_m(u,v)e^{jk\left((u-u_s)x^{i-1}_m+(v-v_s)y^{i-1}_m\right)}\left(1+jk(u-u_s)l^i_m+jk(v-v_s)h^i_m\right). \quad (6)$$

For multibeam optimization, let us also define a vector, $(\boldsymbol{U,V})_{\boldsymbol{SL}}$, which contains the (u,v) values forming the side lobe region for each scanned beam, s

$$(\boldsymbol{U},\boldsymbol{V})_{\boldsymbol{SL}}=\left[(\boldsymbol{u},\boldsymbol{v})_{\boldsymbol{SL},\boldsymbol{1}}\ldots(\boldsymbol{u},\boldsymbol{v})_{\boldsymbol{SL},\boldsymbol{s}}\ldots(\boldsymbol{u},\boldsymbol{v})_{\boldsymbol{SL},\boldsymbol{S}}\right], \quad (7)$$

where the vector contents are determined according to a prespecified main lobe radius, r_b, such that

$$(u,v)\in(\boldsymbol{u},\boldsymbol{v})_{\boldsymbol{SL},\boldsymbol{s}}\,if\,(u-u_s)^2+(v-v_s)^2>r_b^2. \quad (8)$$

Moreover, a minimum allowed inter-element spacing, $d_{\min}$ is defined to prevent element overlapping. To achieve this, the following convex relation[15] must hold for each element pair (α, β)

$$\left(l^i_\alpha-l^i_\beta\right)\left(2x^{i-1}_\alpha-2x^{i-1}_\beta\right)+\left(h^i_\alpha-h^i_\beta\right)\left(2y^{i-1}_\alpha-2y^{i-1}_\beta\right)+\left(x^{i-1}_\alpha-x^{i-1}_\beta\right)^2+\left(y^{i-1}_\alpha-y^{i-1}_\beta\right)^2\geq d^2_{\min}. \quad (9)$$

Consequently, the convex problem to be solved at the i-th iteration of the algorithm is formulated as

$$\min_{\boldsymbol{l}^i,\boldsymbol{h}^i}\rho, s.t.\begin{cases}\max|f^{i,s}_{\boldsymbol{l}^i,\boldsymbol{h}^i}((\boldsymbol{U},\boldsymbol{V}_{\boldsymbol{SL}})|\leq\rho\,\text{for}\forall s,\\ |\boldsymbol{l}^i|\leq\mu,\,|\boldsymbol{h}^i|\leq\mu,\\ (\boxed{9})\text{ holds for}\forall(\alpha,\beta)\end{cases}, \quad (10)$$

where ρ is the maximum SLL, which is simultaneously minimized for all the defined scan positions $s = 1, \ldots, S$. The user defined input parameter μ provides an upper bound for the position perturbations so as to satisfy the linearity approximation in Equation (6). The convex problem given in Equation (10) is a second-order cone program[32] that can be efficiently solved by available solvers (such as CVX[33]).

3 | SIMULATION SETTINGS

In this article, we consider a 5G sector[34] with $a \pm 15/\pm 60$ degree range in elevation/azimuth, which is shown with a red rectangle in the radiation pattern plots. The multibeam optimization is performed for the broadside and sector corners to minimize the maximum SLL within the sector. Note that here we consider that the single sector defines the field-of-view and the radiation outside the sector does not have an impact on the users within the sector. If this is not the case, the SLL minimization can be ≤ performed for the whole visible space: $(u^2 + v^2)1$[15]

A regular, $\lambda/2$-spaced, 8 x 8 square grid array is used as an initial layout. $d_{\min}$ and r_b are set to $\lambda/2$ and 0.2, respectively. μ is taken as 0.08λ for stable convergence. Depending on the order of rotation[4] (=N), only the first slice (1/N-th) of the 8 x 8 array is used in the optimization.

To reduce the computational complexity, a cosθ-type common embedded element pattern is assumed. However, it is possible to include the impact of different element types, mutual coupling, and edge effects into the optimization procedure via performing layout-specific embedded element pattern simulations ($E_m^i(u, v)$ for all m's) at each iteration of the algorithm. The validity of such a strategy has been shown in the literature.[35,36]

Furthermore, considering the Ka-band quad channel analog beamformer chip of NXP Semiconductors,[37] four-element subarray clusters are formed within the optimized slice. Since the aim is to have each cluster as compact as possible (to prevent losses) and to place the chips as far as possible (to have enough space for routing and to reduce coupling) in the integrated array antenna, the "equal-size-k-means" algorithm from ELKI[38] is used. As the result depends on the algorithm initialization, the chip positions and formed clusters are suboptimal. Therefore, two sample (simplified) feed network realizations are given for each optimized layout in Section 4. The ultimate selection has to be made by considering the design limitations.

4 | SIMULATION RESULTS AND DISCUSSION

In this section, the results are grouped and analyzed under three study cases: a fully irregular $M = 64$ element array with no symmetry (used as a benchmark), a quasi-modular $M = 64$ element array with $N = 4$, a quasi-modular $M = 72$ element array with $N = 6$.

4.1 | Fully irregular 64-element array

In this study case, no symmetry is enforced in the layout optimization (i.e., $N = 1$), as previously performed in the literature.[15] The resulting array topology, shown in Figure 1 with the blue circles, becomes fully aperiodic, with the lowest possible SLL, but the highest design complexity due to the complete irregularity. In fact, once the equal-size-k-means clustering algorithm is performed on the positions of the beamformer chips, it is seen that such a topology requires 16 different unique four-element subarray clusters, with the chips located at the red circles in Figure 1, which shows two candidate suboptimal layout configurations.

For the optimized topology, the (normalized) broadside and corner beam radiation patterns are given in Figure 2. In the case of the broadside beam, the maximum SLL within the sector is 25.2 dB below the maximum directivity of 24.4 dBi. For the corner beam, the maximum SLL within the sector is 21.8 dB below the maximum directivity of 20.1 dBi. The convergence to the minimized SLL is reached in 50 iterations by using small element position perturbations

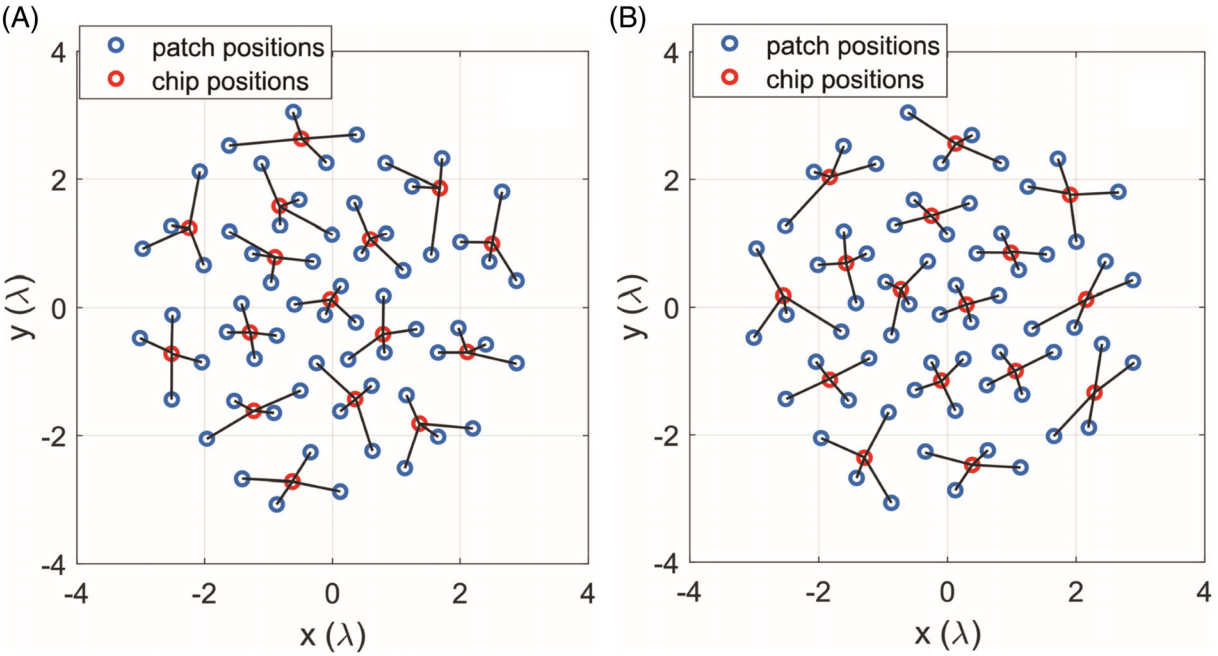

FIGURE 1 Sample suboptimal subarray clusters for the fully irregular 64-element array: (A) option #1 and (B) option #2 [Color figure can be viewed at wileyonlinelibrary.com]

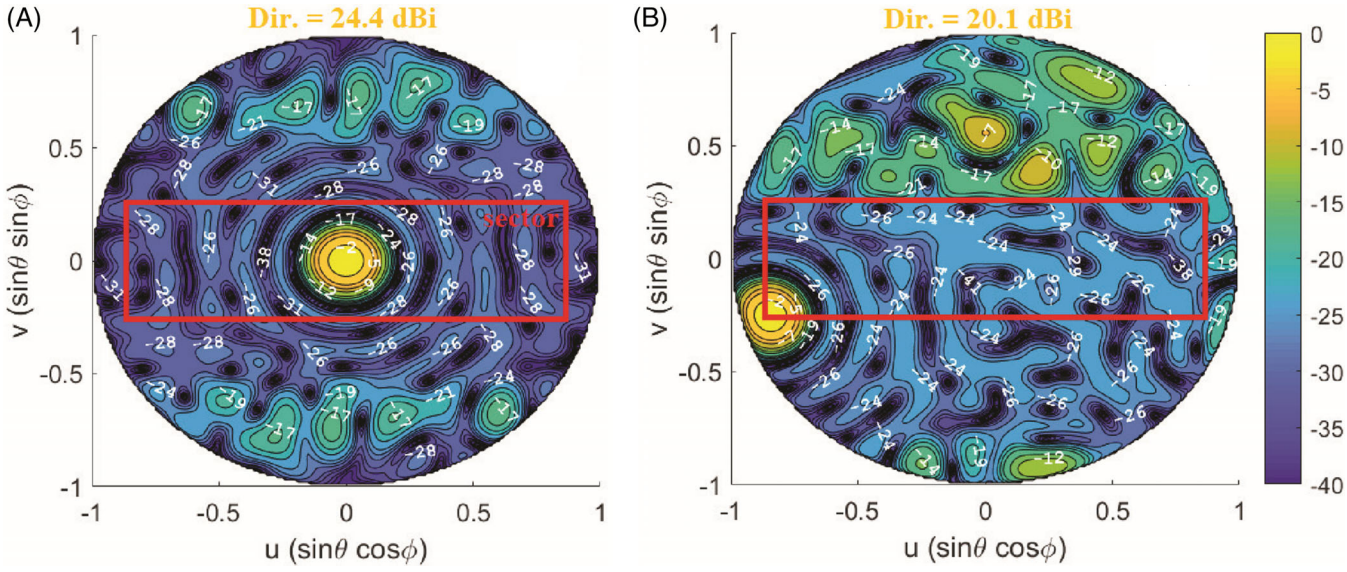

FIGURE 2 Multibeam radiation patterns (in dB, normalized with respect to the maximum beam directivity) of the optimized fully irregular 64-element array: (A) $u_s = 0$, $v_s = 0$ and (B) $u_s = -\sin\pi/3$, $v_s = -\sin\pi/12$ [Color figure can be viewed at wileyonlinelibrary.com]

at each iteration as explained in Section 2, using the periodic, $\lambda/2$-spaced, 8 x 8 square grid array is used as the initial layout.

With the introduction of the (quasi-)modularity, the aim in this article is to reduce the number of unique subarray clusters for design/fabrication/calibration simplicity, while still keeping a relatively low-maximal SLL inside the communication sector.

4.2 | Quasi-modular 64-element array with $N = 4$

In this case, 1/4-th of the initial 8 x 8 element array (with 16 elements in the first quadrant) is optimized and sequential rotation is used. The resulting antenna array and possible suboptimal chip layouts are provided in Figure 3. It is worth of note that the different colors in the four-element subarrays

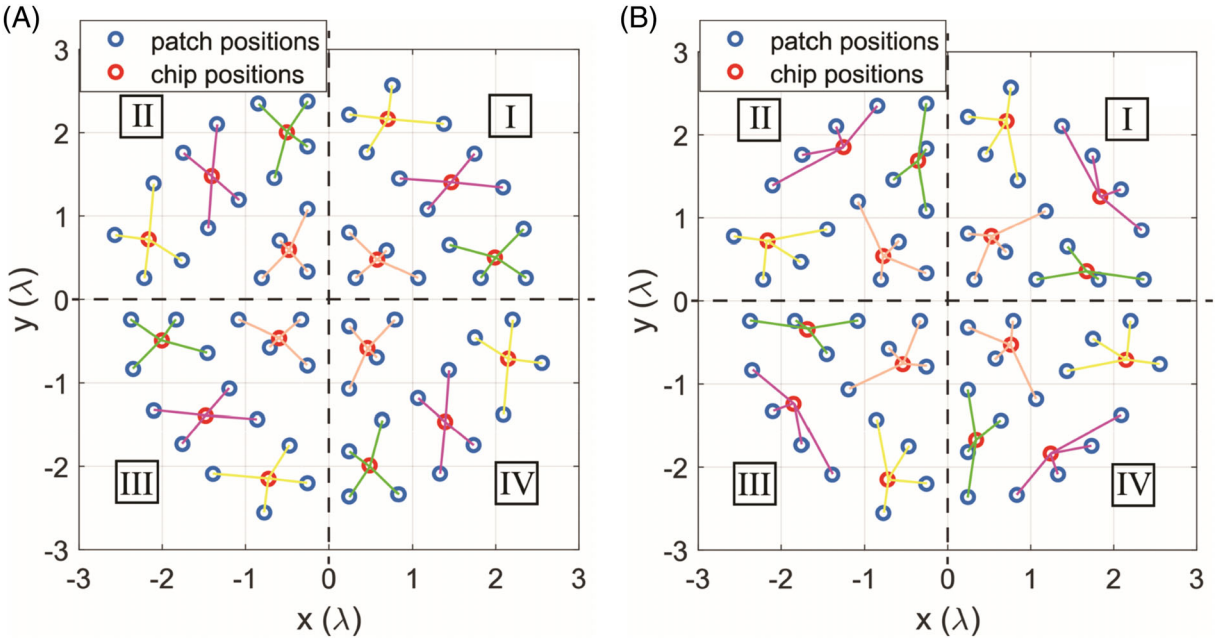

FIGURE 3 Sample suboptimal subarray clusters for the quasi-modular 64-element array: (A) option #1 and (B) option #2 [Color figure can be viewed at wileyonlinelibrary.com]

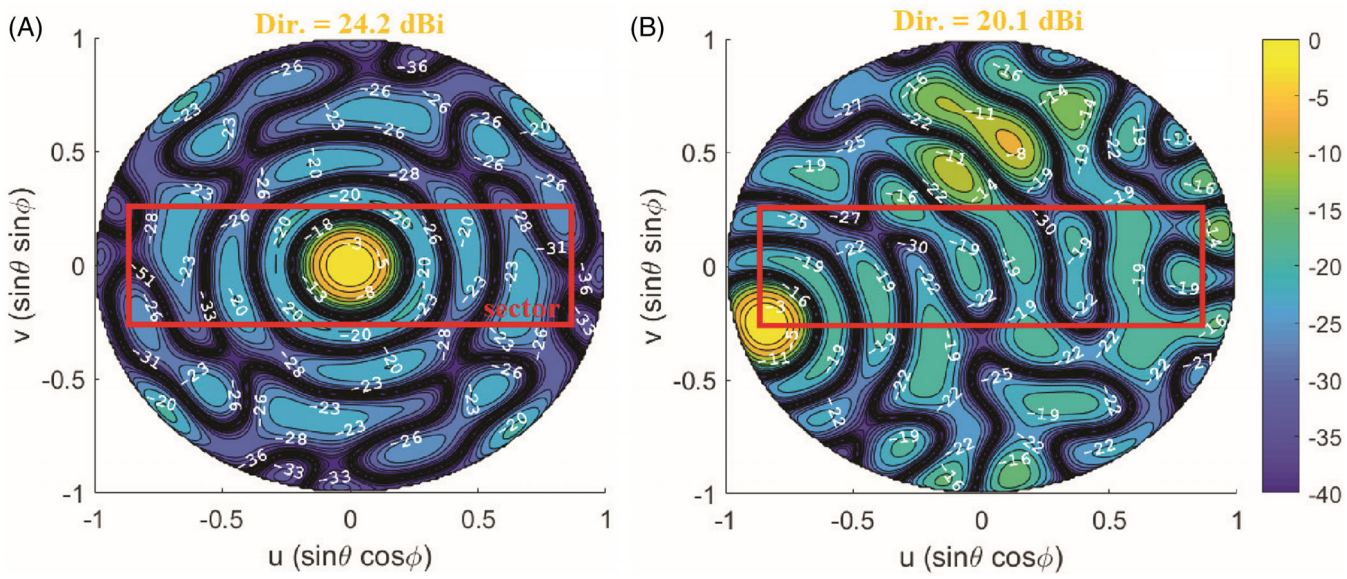

FIGURE 4 Multibeam radiation patterns (in dB, normalized with respect to the maximum beam directivity) of the optimized quasi-modular 64-element array: (A) $u_s = 0$, $v_s = 0$ and (B) $u_s = -\sin\pi/3$, $v_s = -\sin\pi/12$ [Color figure can be viewed at wileyonlinelibrary.com]

in Figure 3 represent the unique subarray clusters that are repeated rotationally. It can be seen that only four different clusters are required due to the fourth order rotational symmetry.

The increased simplification in design comes at the expense of the increased side lobes. For the optimized topology in this part, the (normalized) broadside and corner beam radiation patterns are given in Figure 4. In the case of the broadside beam, the maximum SLL within the sector is 19.8 dB below the maximum directivity of 24.2 dBi. For the corner beam, the maximum SLL within the sector is 16.2 dB below the maximum directivity of 20.1 dBi. In this case, the convergence to the minimized SLL is reached in 12 iterations.

4.3 | Quasi-modular 72-element array with $N = 6$

In the last case, only 1/6-th of the initial 8 x 8 element array (12 elements in the first slice) is optimized and sequential rotation is applied. The resulting antenna array and possible sub-optimal chip layouts are provided in Figure 5. The

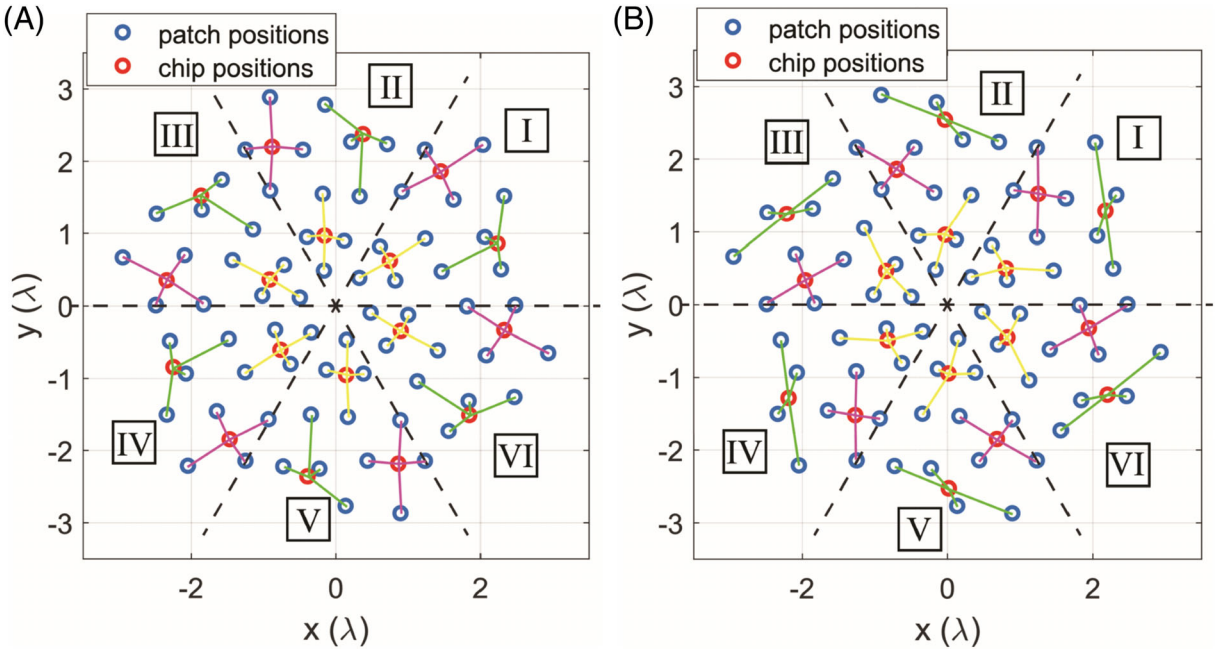

FIGURE 5 Sample suboptimal subarray clusters for the quasi-modular 72-element array: (A) option #1 and (B) option #2 [Color figure can be viewed at wileyonlinelibrary.com]

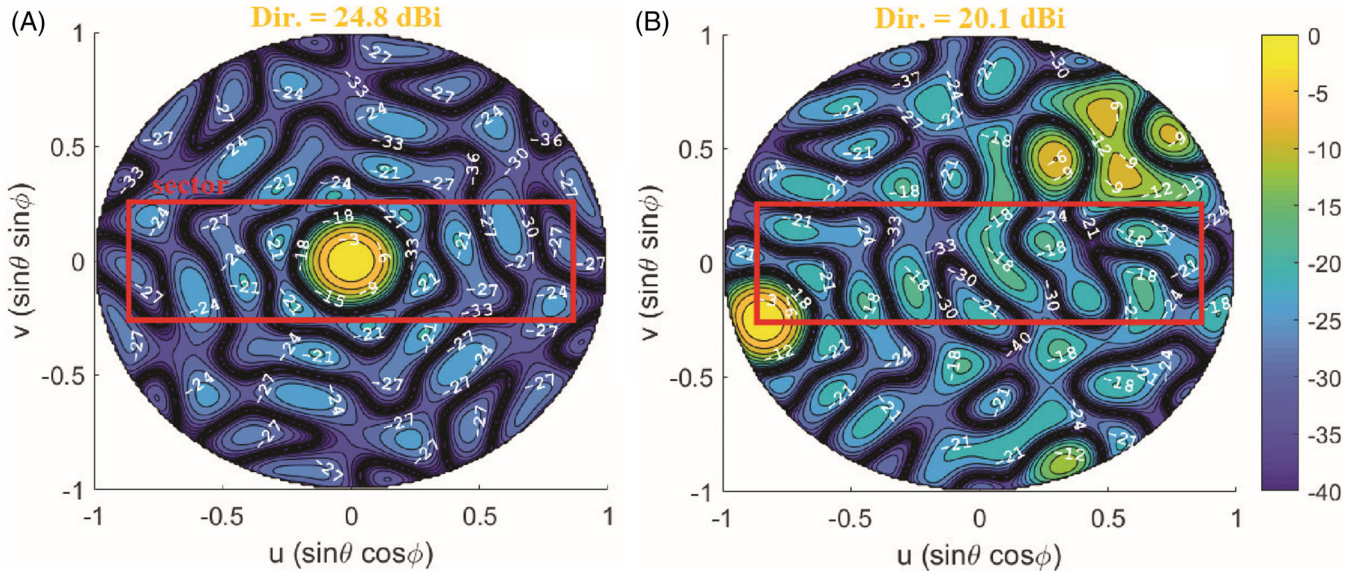

FIGURE 6 Multibeam radiation patterns (in dB, normalized with respect to the maximum beam directivity) of the optimized quasi-modular 72-element array: (A) $u_s = 0$, $v_s = 0$ and (B) $u_s = -\sin\pi/3$, $v_s = -\sin\pi/12$ [Color figure can be viewed at wileyonlinelibrary.com]

element number increases from 64 to 72. Similarly, the number of chips increases from 16 to 18. However, now, only three unique subarray clusters are needed.

For the optimized topology in this part, the (normalized) broadside and corner beam radiation patterns are given in Figure 6. In the case of the broadside beam, the maximum SLL within the sector is 20.5 dB below the maximum directivity of 24.8 dBi. For the corner beam, the maximum SLL within the sector is 17.0 dB below the maximum directivity of 20.1 dBi.

The convergence to the minimized SLL is reached only in seven iterations. Thus, faster convergence is achieved with increased order of symmetry, which comes in addition to the much reduced computational complexity as compared to the fully irregular array. As seen from the radiation patterns, the price to pay is the increased maximal SLL, which is higher by about 5 dB, as compared to the one of the fully irregular array discussed in Section 4.1.

Note that the SLL suppression performance will improve further for larger arrays as the degree of design freedom

increases, which comes at the expense of increased computation time/resources and design complexity. To deal with that, a higher order of rotational symmetry can be used for the larger arrays, by compromising from the SLL reduction capability to some extent. Another option is to change the solver type in CVX and instead of the self-dual minimization solver, to use, for example, the splitting conic solver, which is designed to solve large problems, but to more modest levels of accuracy.[33]

5 | CONCLUSION

The synthesis of quasi-modular, CP integrated multibeam 5G base station antennas with relatively low SLLs has been studied to ease the fabrication and circuit routing requirements of the fully aperiodic arrays that were previously proposed in the literature.[15] Only a small portion of the whole array has been used in an iterative convex layout optimization routine, which has been combined with (i) the equal-size-k-means clustering algorithm to form the sub-optimal subarray clusters and (ii) the sequential rotation technique to achieve modularity.

Through the simulations, it has been seen that the proposed quasi-modular arrays provide a good compromise between the side lobe performance and the design/fabrication complexity.

Note that, with the proper patch center adjustments, the same algorithm can also be straightforwardly used to synthesize low-sidelobe LP arrays having a rotationally symmetric feed network.

The realization and testing of the chip-integrated arrays with proper design of the feeding, circuit routing and calibration remain as a future work.

ACKNOWLEDGMENTS

This work was supported in part by NWO and in part by NXP Semiconductors in the framework of the partnership program on advanced 5G solutions within the project number 15590 entitled "Antenna Topologies and Front-end Configurations for Multiple Beam Generation."

ORCID

Yanki Aslan https://orcid.org/0000-0002-6834-8375

ENDNOTES

[1]The array power efficiency is defined as the ratio of the peak power density of the phase (and/or amplitude) tapered array to the peak power density of the uniformly excited array with progressive phase shifts defined by the scan angle.

[2]The first slice here is defined as the region within the first quadrant of the Cartesian plane where both x and y coordinates of the array elements are positive. The edges of the slice are on the positive parts of the x-axis and the $y = x\tan(2\pi/N)$ line.

[3]At each iteration of the algorithm, the previously obtained and known element locations are used. Only the first iteration is an exception for which an initial set of locations at the first slice must be predefined.

[4]The order of rotation, N, denotes the total number of periodically repeated slices used in the rotationally symmetric layout. The angular width of each slice is $2\pi/N$ radians. The overall layout coincides with itself when the angle of rotation is an integer multiple of $2\pi/N$ radians.

REFERENCES

[1] Magri H, Abghour N, Ouzzif M. Key concepts of 5th generation mobile technology. *WASET IJECE*. 2015;9(4):471-474.

[2] Morabito AF, Massa A, Rocca P, Isernia T. An effective approach to the synthesis of phase-only reconfigurable linear arrays. *IEEE Trans Antennas Propag*. 2012;60(8):3622-3631.

[3] Liu Y, Jiao YC, Zhang YM, Tan YY. Synthesis of phase-only reconfigurable linear arrays using multiobjective invasive weed optimization based on decomposition. *Int J Antennas Propag*. 2014; 2014:1-11.

[4] Aslan Y, Puskely J, Roederer A, Yarovoy A. Phase-only control of peak sidelobe level and pattern nulls using iterative phase perturbations. *IEEE Antennas Wireless Propag Lett*. 2019;18(10): 2081-2085.

[5] Prisco G, D'Urso M. Maximally sparse arrays via sequential convex optimizations. *IEEE Antennas Wireless Propag Lett*. 2012;11: 192-195.

[6] Gies D, Rahmat-Samii Y. Particle swarm optimization for reconfigurable phase-differentiated array design. *Microwave Opt Technol Lett*. 2003;38(3):172-175.

[7] Liu Y, Liu QH, Nie Z. Reducing the number of elements in multiple-pattern linear arrays by the extended matrix pencil methods. *IEEE Trans Antennas Propag*. 2014;62(2):652-660.

[8] Bucci OM, D'Urso M, Isernia T, Angeletti P, Toso G. Deterministic synthesis of uniform amplitude sparse arrays via new density taper techniques. *IEEE Trans Antennas Propag*. 2010;58(6):1949-1958.

[9] Jain R, Mani GS. Dynamic thinning of antenna array using genetic algorithm. *Prog Electromagn Res B*. 2011;32:1-20.

[10] Liu Y, You P, Zhu C, Tan X, Liu QH. Synthesis of sparse or thinned linear and planar arrays generating reconfigurable multiple real patterns by iterative linear programming. *Prog Electromagn Res*. 2016;155:27-38.

[11] Haupt RL. Adaptively thinned arrays. *IEEE Trans Antennas Propag*. 2015;63(4):1626-1632.

[12] Bucci OM, Perna S, Pinchera D. Synthesis of isophoric sparse arrays allowing zoomable beams and arbitrary coverage in satellite communications. *IEEE Trans Antennas Propag*. 2015;63(4): 1445-1457.

[13] Fuchs B, Skrivervik A, Mosig JR. Synthesis of uniform amplitude focused beam arrays. *IEEE Antennas Wireless Propag Lett*. 2012; 11:1178-1181.

[14] Aslan Y, Puskely J, Roederer A, Yarovoy A. Synthesis of multiple beam linear arrays with uniform amplitudes. In Proceedings of 12th EuCAP. IEEE. London, UK; 2018

[15] Aslan Y, Puskely J, Roederer A, Yarovoy A. Multiple beam synthesis of passively cooled 5G planar arrays using convex optimization. *IEEE Trans Antennas Propag*. 2019;68(5):3557-3566.

[16] Aslan Y, Puskely J, Roederer A, Yarovoy A. Trade-offs between the quality of service, computational cost and cooling complexity in interference-dominated multi-user SDMA systems. *IET Comm*. 2019;14(1):144-151.

[17] Aslan Y, Puskely J, Janssen J, Geurts M, Roederer A, Yarovoy A. Thermal-aware synthesis of 5G base station antenna arrays: an overview and a sparsity-based approach. *IEEE Access*. 2018;6: 58868-58882.

[18] Makino S, Kadoguchi S, Betsudan Si, et al An aperiodic array antenna using diamond tiles as subarrays. In Proceedings of 3rd EuCAP IEEE; 2009: 3479–3482.

[19] Pierro V, Galdi V, Castaldi G, Pinto IM, Felsen LB. Radiation properties of planar antenna arrays based on certain categories of aperiodic tilings. *IEEE Trans Antennas Propag*. 2005;53(2): 635-644.

[20] Rocca P, Anselmi N, Polo A, Massa A. An irregular two-sizes square tiling method for the design of isophoric phased arrays. *IEEE Trans Antennas Propag*. 2020;68(6):4437-4449.

[21] Xiong ZY, Xu ZH, Xiao SP. Beamforming properties and design of the phased arrays in terms of irregular subarrays. *IET Microw Antennas Propag*. 2014;9(4):369-379.

[22] Dong W, Xu ZH, Liu XH, Xiao SP, et al. Irregular subarray tiling via heuristic iterative convex relaxation programming. *IEEE Trans Antennas Propag*. 2019;68(4):2842-2852.

[23] Alshammary A, Weiss S, Almorqi S. Grating lobe suppression in rotationally tiled arrays. In Proceedings of 11th EuCAP. IEEE; 2017: 1158–1161.

[24] Bencivenni C, Ivashina MV, Maaskant R, Wettergren J. Synthesis of maximally sparse arrays using compressive sensing and full-wave analysis for global earth coverage applications. *IEEE Trans. Antennas Propag*. 2016;64(11):4872-4877.

[25] Teshirogi T, Tanaka M, Chujo W. Wideband circularly polarised array antenna with sequential rotations and phase shift of elements. In Proceedings of ISAP Tokyo, Japan: 1985 117–120.

[26] Huang J. A technique for an array to generate circular polarization with linearly polarized elements. *IEEE Trans Antennas Propag*. 1986;AP-34(9):1113-1124.

[27] Roederer AG. Some comments on the gain of large planar arrays. *IEEE Antennas Propag Soc Newslet*. 1989;31(5):63-64.

[28] Luo Q, Gao S, Sobhy M, et al. Dual circularly polarized equilateral triangular patch array. *IEEE Trans Antennas Propag*. 2016; 64(6):2255-2262.

[29] Smolders AB, Johannsen U. Axial ratio enhancement for circularly-polarized millimeter-wave phased-arrays using a sequential rotation technique. *IEEE Trans Antennas Propag*. 2011;59(9):3465-3469.

[30] Hu YJ, Ding WP, Cao WQ. Broadband circularly polarized microstrip antenna array using sequentially rotated technique. *IEEE Antennas Wireless Propag Lett*. 2011;10:1358-1361.

[31] Smolders AB. Random sequential rotation: A new technique for sidelobe control of circularly-polarized phased arrays. In Proceedings of IEEE APS-URSI. Memphis, TN; 2014.

[32] Alizadeh F, Goldfarb D. Second-order cone programming. *Math Program*. 2003;95(1):3-51.

[33] Grant M, Boyd S. CVX: Matlab Software for Disciplined Convex Programming, Version 2.1. http://cvxr.com/cvx; 2014.

[34] Degirmenci E. EMF Test Report: Ericsson AIR 5121. Tech. Rep. GFTB-17:001589 Uen Rev B, Ericsson AB; Stockholm, Sweden: 2018.

[35] Aslan Y, Candotti M, Yarovoy A. Synthesis of multi-beam space-tapered linear arrays with side lobe level minimization in the presence of mutual coupling. In Proceedings 13th EuCAP Krakow, Poland, 2019.

[36] Van HB, Jha SN, Craeye C. Fast full-wave synthesis of printed antenna arrays including mutual coupling. *IEEE Trans Antennas Propag*. 2016;64(12):5163-5171.

[37] Aslan Y, Kiper CE, Biggelaar V., Johannsen U., Yarovoy A. Passive cooling of mm-wave active integrated 5G base station antennas using CPU heatsinks. In Proceedings of 16th EuRAD Paris, France; 2019; 121–124.

[38] Schubert E, Zimek A. ELKI: a large open-source library for data analysis - ELKI release 0.7.5 "Heidelberg". *CoRR*. 2019; abs/1902.03616. http://arxiv.org/abs/1902.03616

How to cite this article: Aslan Y, Puskely J, Roederer A, Yarovoy A. Synthesis of quasi-modular circularly polarized 5G base station antenna arrays based on irregular clustering and sequential rotation. *Microw Opt Technol Lett*. 2020;1–8. https://doi.org/10.1002/mop.32735